15th World Congress on Computational Mechanics (WCCM-XV)
8th Asian Pacific Congress on Computational Mechanics (APCOM-VIII)
Virtual Congress: 31 July – 5 August 2022
S. Koshizuka (Ed.)

CODE-ORIENTED FLOOR ACCELERATION RESPONSE SPECTRA OF RC FRAMED BUILDINGS ACCOUNTING FOR NONLINEAR RESPONSE OF MASONRY INFILLS

FABIO MAZZA[1] AND ANGELO DONNICI[2]

[1]Università della Calabria (Italy)
87036 Rende (CS)
fabio.mazza@unical.it

[2] Università della Calabria (Italy)
87036 Rende (CS)
angelo.donnici@unical.it

Key words: Floor Acceleration Response Spectra, RC Framed Buildings, Masonry Infills, In-Plane and Out-Of-Plane Response, Nonlinear Seismic Analysis.

Abstract. *Modern code-oriented elastic floor response spectra formulations for RC framed structures do not take into account effects of non-negligible nonstructural components in terms of mass and stiffness, such as masonry infills (MIs). MIs nonlinear behaviour can be represented through the combination and mutual interaction between the in-plane (IP) and out-of-plane (OOP) responses. The present work is aimed at identifying the effect of IP and OOP nonlinear modelling assumptions on floor acceleration response spectra, consistently with the required seismic intensity level for simplified verification of life-threatening nonstructural elements. To this end, a spatial one-bay multi-storey shear-type model is considered as equivalent to infilled RC framed buildings with common double-leaf MIs. Additional variability of the following design parameters is considered: number of storeys (three, five and seven); behaviour factor (low, 1.5, medium, 3, and high, 4.5); OOP strength of MIs, with lower and upper bound values corresponding to one- and two-way arching mechanisms, respectively. A recently proposed computer code, that includes a five-element nonlinear infill macro-model comprising four diagonal OOP beams and one (horizontal) central IP truss, is considered for the numerical investigation. The proposed algorithm modifies stiffness and strength values of MIs in the OOP direction on the basis of simultaneous or prior IP damage and vice versa. Moreover, a lumped plasticity model describes the inelastic behaviour of RC frame members. Biaxial spectrum-compatible accelerograms are considered at life-safety limit state provided by the Italian seismic code. A simplified code-oriented formulation for the evaluation of floor response spectra of infilled RC framed structures is proposed. Nonstructural maximum acceleration is firstly evaluated by means of vertical and nonstructural amplification factors. Continuous wavelet transforms are used to calibrate parameters that define the resonance region width, accounting for moving resonance due to nonlinearity and higher modes effects. Parabolic and Gaussian curves are considered in order to reproduce pre- and post-resonance regions, respectively. Finally, a code-oriented proposal is compared to exact elastic and inelastic floor spectra of MIs evaluated over their common range of OOP vibration periods.*

1 INTRODUCTION

Masonry infills (MIs) are the most common Italian and European nonstructural elements in RC buildings. Their damage and potential collapse in the out-of-plane (OOP) direction may be life-threatening. Floor response spectra are the most effective tools to predict OOP accelerations at different structural heights so as to carry out safety verification of nonstructural components. Rigorous floor spectral acceleration evaluation is usually a demanding task, that relies on a decoupled structural-nonstructural analysis assumption and may be heavily affected by seismic input. Alternative spectrum-to-spectrum approaches (e.g. see [1] and [2]) are based on the conversion of ground spectrum to floor one through modal superposition, however their use is still limited. Actually, many seismic codes (e.g. NTC18 [3], EC8 [4], ASCE-SEI 41/17 [5] and NZS1170 [6]) provide even more simplified formulations to practitioners, neglecting higher modes participation on nonstructural elements seismic motion. Code-based floor spectra are usually described by simple curves, where the maximum acceleration value depends on in-height and nonstructural amplification parameters. In-plane (IP) and out-of-plane (OOP) effects of MIs on floor response spectra of acceleration have been poorly investigated, due to the lack of low demanding up-to-date macro-models that could be used to carry out extensive parametric analyses [7]. A general procedure to derive code-oriented floor spectra is presented in this work. The first step consists in the generation of simplified nonstructural models, that take into account the effect of MIs on the seismic behaviour of a reinforced concrete (RC) benchmark structure. A wide set of variabilities is assigned to models and a bidirectional seismic input, consistent with OOP nonstructural stability verification limit state, is assigned to each model. Nodal acceleration time histories are post-processed to evaluate exact floor response spectra as well as dominant frequencies through wavelet transform [8]. Similarly, maximum MIs OOP accelerations are collected to generate accurate MIs elastic and inelastic spectra. The simplified formulation parameters are calibrated on the basis of parametric results. Lastly, a preliminary validation procedure on exact MIs floor spectra is discussed.

2 INFILLED TEST STRUCTURES

2.1 Layout and design of RC framed benchmark structures

A three-dimensional one-bay multi-storey nonlinear shear-type benchmark model is assumed to carry out nonlinear dynamic analyses (Fig. 1). Each RC structure has a square plan, with bay length L = 5.5m, and is fully infilled. An interstorey height h = 3m and a constant floor mass m^* are assumed. The floor mass value is based on floor mass-to-floor stiffness equivalence between real multi-bay multi-storey framed structures and benchmark model [9]. The design philosophy of RC frames is consistent with the typical Italian building stock and based on low seismic design requirements (i.e. no strength hierarchy between structural elements). Three total building heights H, corresponding to 3, 5 and 7 storey structures, are considered, in order to investigate the fundamental period T_1 variability. Seismic design forces are evaluated assuming three behaviour factor values: 1.5 (low ductility, LD), 3.0 (medium ductility, MD) and 4.5 (high ductility, HD). RC beams and columns are modelled through lumped plasticity elements. All types of masonry infill seismic behaviour are investigated: elastic IP-elastic OOP ($E_{IP}E_{OOP}$) and inelastic IP-elastic OOP ($I_{IP}E_{OOP}$), without IP-OOP interaction, inelastic IP-

inelastic OOP with single interaction ($I_{IP} \rightarrow I_{OOP}$) and inelastic IP-inelastic OOP with mutual interaction ($I_{IP} \leftrightarrow I_{OOP}$).

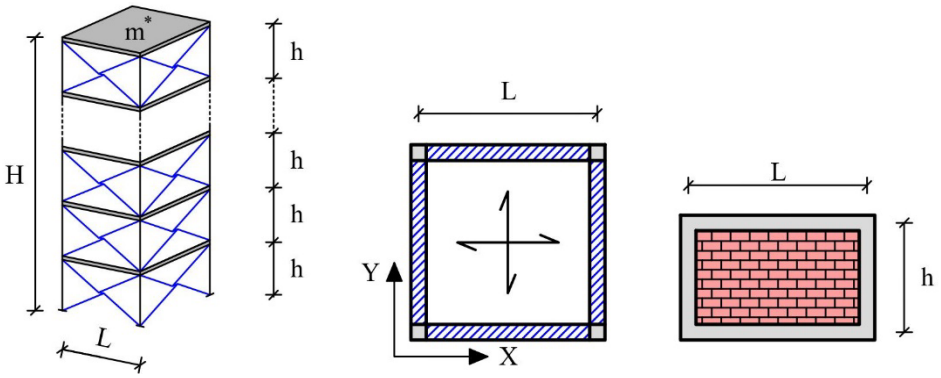

Figure 1: RC benchmark structure layout.

2.2 Nonlinear modelling of masonry infills

A five element macro-model represents each masonry infill [7]. The IP inelastic response is assigned to the central element (Fig. 2a), that behaves as nonlinear truss, with stiffness $k_{wi}^{(IP)}$ and distributed IP mass $\mu^{(IP)}$. OOP behaviour is governed by the combined OOP stiffness ($k_{wi}^{(OOP)}$) of diagonal beam elements (Fig. 2b), rigidly connected through the central one. A concentrated OOP mass equal to 81% of the total panel mass is split between the two central nodes, representing the effective mass related to main OOP modal shape. An internal routine of a home-made computer code, based on IP or OOP damage threshold exceedance, handles the IP or OOP backbone update, depending on the level of OOP actions or IP drift experienced by the panel. Additional and more detailed information can be found in [7], [9] and [10].

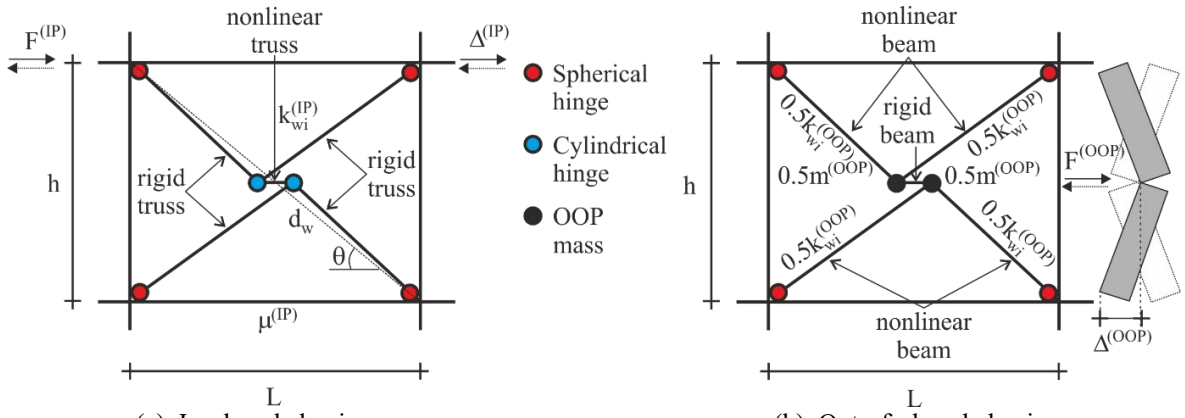

(a) In-plane behaviour. (b) Out-of-plane behaviour.

Figure 2: Masonry infill macro-model.

A trilinear IP backbone is calculated following the procedure discussed in [9], assuming a typical double layer (12cm + 12cm) hollow brick masonry infill. This backbone is kept constant among seismic analyses, since its variability would affect only the fundamental period T_1 (that is already taken into account). A bilinear OOP backbone curve is assigned to each MI, adopting

upper (FEMA 356 [11], F) and lower (Dawe & Seah [12], DS) bound formulations for the OOP maximum strength. In this way, the effect of a wide range of possible OOP damage states as well as different OOP→IP interaction degrees is investigated. Ten OOP backbone curves are computed (Fig. 3), varying the initial branch stiffness to match specific OOP vibration period values, within a realistic range for MIs ($T_1^{(OOP)}$=0-0.3s, [13]). Therefore, MIs nodal maximum OOP acceleration values from dynamic analyses will be assembled into exact MIs floor spectra. Single (IP→OOP) and mutual (IP↔OOP) interaction backbone decay laws are suggested in [9], based on Ricci et al. [14] and Al-Chaar [15] formulations, respectively.

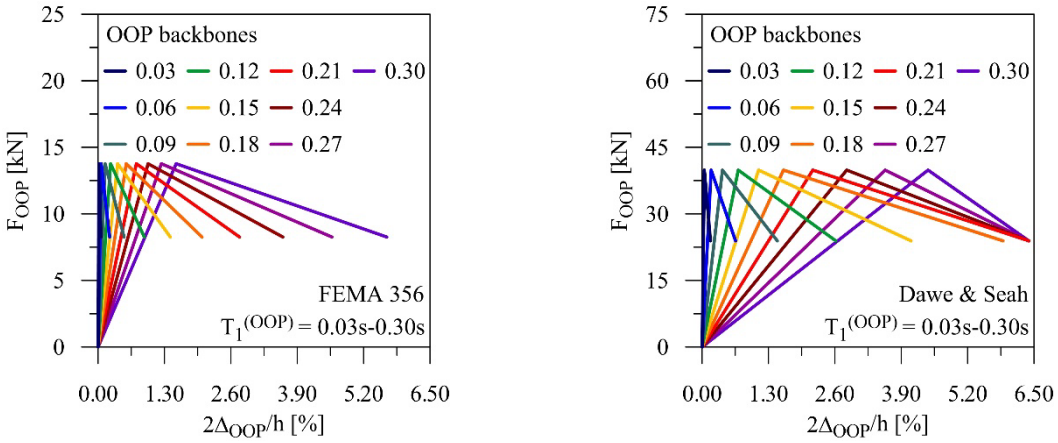

(a) FEMA 356 [9]. (b) Dawe & Seah [10].

Figure 3: Parametric OOP backbone curves.

2.3 Ground motion selection

One pair of bidirectional artificial ground motions, previously discussed in [9], is selected to match Life Safety (LS) elastic ground spectrum of acceleration. These motions are evaluated in compliance with NTC18 [3], assuming the LS intensity level (PGA_{LS}=0.262g) consistent with the required OOP stability check of nonstructural elements. A continuous wavelet transform analysis of generated accelerograms guarantees that the overall frequency content matches the fundamental period range of the designed benchmark models. This procedure is of paramount importance to justify, in this preliminary stage, the use of a single pair of seismic inputs, as the amplification of structural accelerations due to frequency similarity will replicate peak response values that would result from spectrum-compatible real seismic input set.

3 NUMERICAL RESULTS

Nonlinear time histories (NLTHs) results referred to different number of storeys are represented in terms of relative height (z/H) in order to derive general trends that will guide the calibration of code-oriented parameters. In the same way, exact floor spectra are normalized by the fundamental period T_1 of the associated bare frame structure, offering a convenient way to evaluate and compare nonstructural acceleration amplification ranges between sets of variabilities. A comparison between code expressions (Italian NTC18 [3], European EC8 [4], American ASCE-SEI 41/17 [5], New Zealand NZS1170 [6]) and envelope curves for spectrum parameters will be discussed too, when applicable.

3.1 Floor amplification factor

The floor amplification factor a_H is intended as the ratio between Peak Floor Acceleration (*PFA*) and Peak Ground Acceleration (*PGA*). Mean values are preliminarily obtained for each fixed number of storeys. Envelopes are derived afterwards, differentiating curves on the basis of MI model assumption and ductility class (Fig. 4a/b/c).

As expected lower structural damage and higher in-height amplification correspond to lower values of the behaviour factor q. The upper bound curves are related to elastic MIs in both IP and OOP directions while lower bound ones refer to inelastic IP-OOP behaviour, with mutual interaction and FEMA 356 OOP strength formulation. In this last case, MIs are heavily damaged and structural behaviour tends to that observed for the bare frame. A tendency toward linear amplification is typical of LD structures (Fig. 4a), while curves become gradually flattened as behaviour factor increases (Fig. 4b/c). NZS1170 formulation depends on absolute heights, therefore curves are evaluated for all three total heights; constant branches are referred to higher structures (i.e. 5 and 7 storeys). NZS1170 expression for seven-storey structures seems to be compatible with LD trends (Fig 4a), while NTC18 one is the closest to HD mean values (Fig 4c).

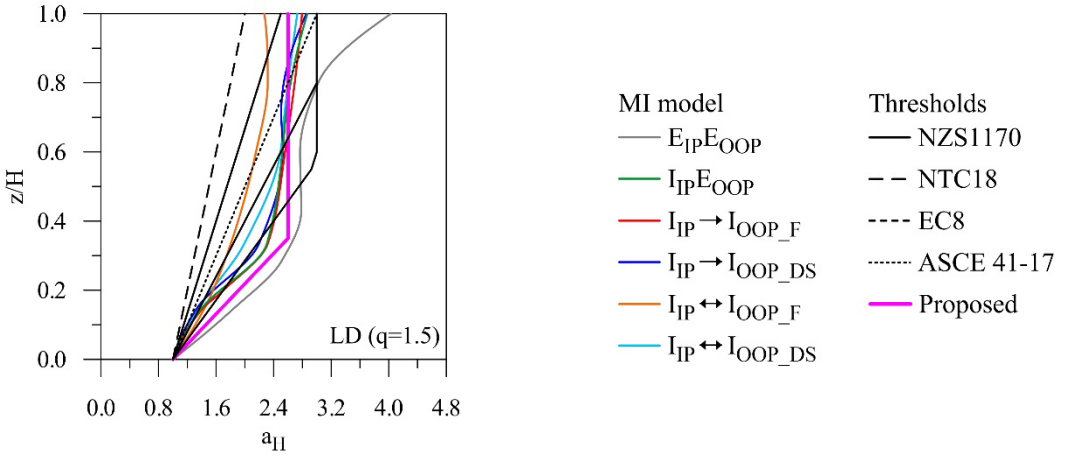

(a) Low ductility class (LD).

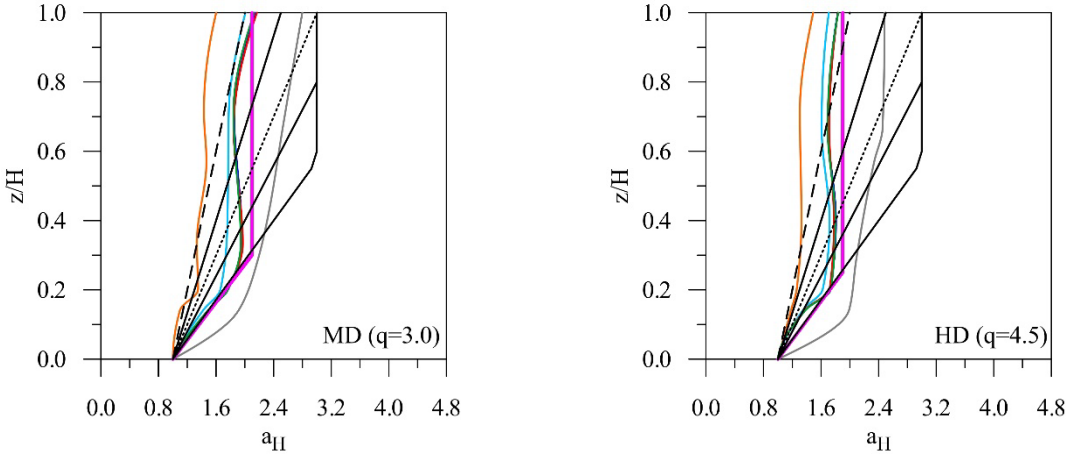

(b) Medium ductility class (MD).

(c) High ductility class (HD).

Figure 4: Comparison between NLTH results, code-based thresholds and proposed expressions for a_H.

3.2 Nonstructural amplification factor

The nonstructural (NS) amplification factor a_{NS} can be defined as the ratio between maximum nonstructural acceleration $S_a(T_{NS})_{max}$, identified for each exact floor response spectrum (ξ_{NS} = 5%), and the associated floor maximum acceleration (*PFA*). The a_{NS} range of values mainly depends on the structural behaviour factor (Fig. 5a/b/c), with higher values for LD structures (Fig. 5a). Curves referred to different MIs IP-OOP modelling assumptions show a linear tendency, that experiences modest increase as structural inelasticity spreads out (Fig. 5b/c). A very limited dispersion of values between envelopes can be noticed, when compared to a_H trends, therefore no evident upper or lower bound assumption stands out. Amplification parameters from different codes do not depend on structural behaviour factor. NZS1170, EC8 and ASCE-SEI 41/17 predictions heavily underestimate NS amplification, with increasing relative height *z/H* of the nonstructural element. NTC18 constant value is generally closer to observed values at upper storeys of MD and HD structures (Fig. 5b/c), with a general overestimation at bottom ones. The linear trend of LD amplification coefficient is averaged by the NTC18 one, along the building height.

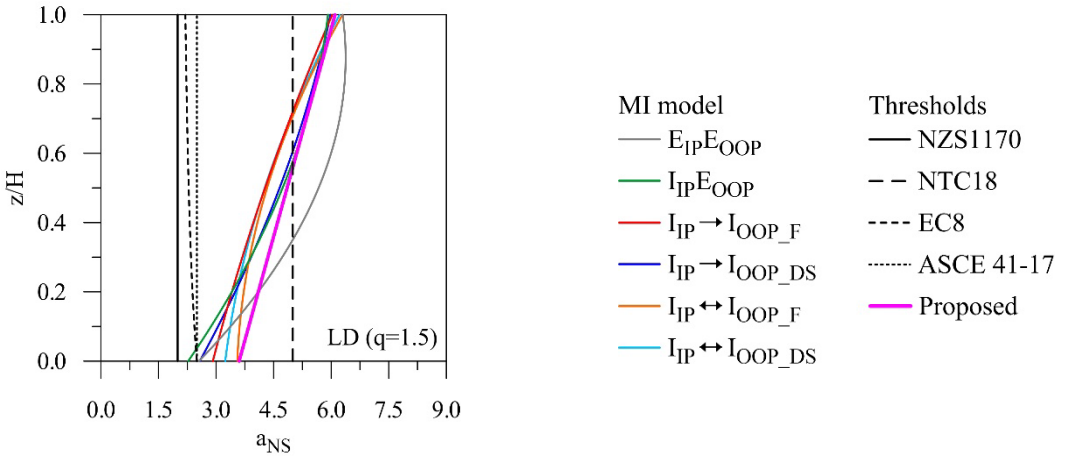

(a) Low ductility class (LD).

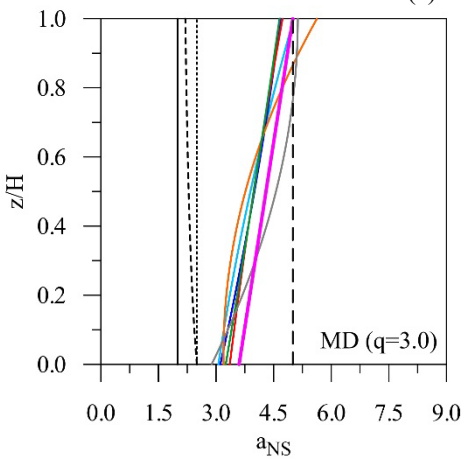

(b) Medium ductility class (MD).

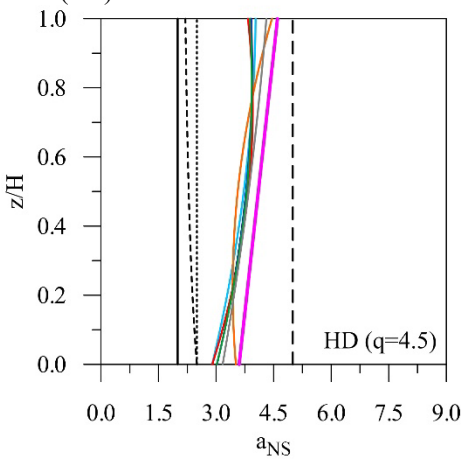

(c) High ductility class (HD).

Figure 5: Comparison between NLTH results, code-based thresholds and proposed expressions for a_{NS}.

3.3 Effects of higher modes

Continuous wavelet transforms (CWTs) of floor acceleration nodal time histories provide useful and clear information about dominant frequencies.

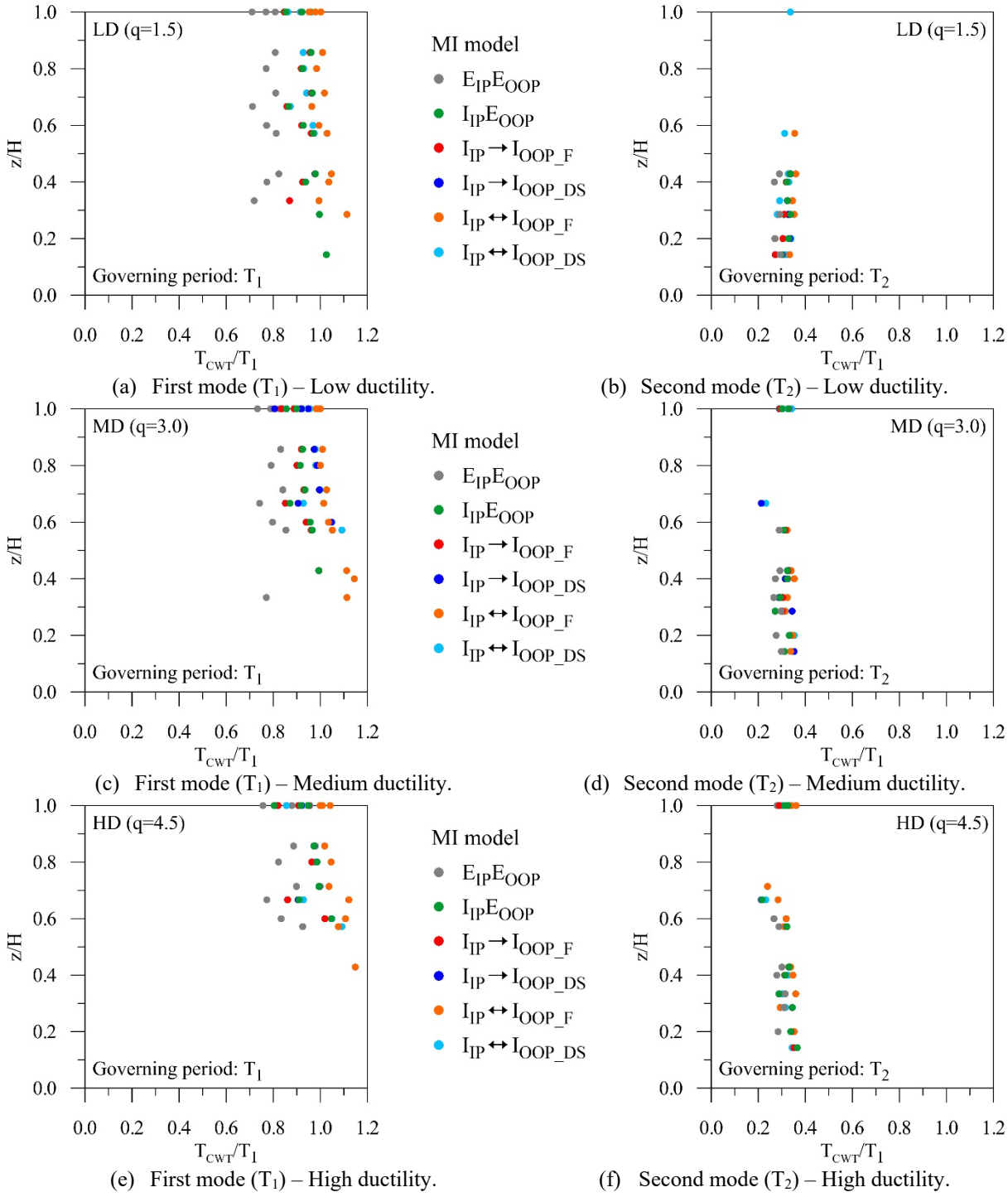

(a) First mode (T_1) – Low ductility. (b) Second mode (T_2) – Low ductility.

(c) First mode (T_1) – Medium ductility. (d) Second mode (T_2) – Medium ductility.

(e) First mode (T_1) – High ductility. (f) Second mode (T_2) – High ductility.

Figure 6: Spatial distribution of dominant periods.

For each structure, reference elastic fundamental period of vibration T_1 is evaluated through modal analysis so as to normalise the obtained dominant values. In this way, structural periods elongation due to structural and nonstructural nonlinear behaviour can be quantified. Figure 6 summarises the distribution along the building height of frequencies with the highest CWT coefficients. The fundamental period T_1 has a strong impact on structural accelerations at higher storeys (Fig. 6a/c/e) while the second translational period T_2 dominates lower ones (Fig. 6b/d/f). The influence of T_2 extends to upper storeys in the case of higher q values, confirming that structural damage heavily affects the fundamental period T_1 contribution (Fig. 6e).

4 CODE-ORIENTED FLOOR SPECTRA

Results presented in Section 3 provide all the information necessary to calibrate a code-oriented formulation for elastic floor spectra of acceleration at LS limit state. The EIP-EOOP infill response assumption will not be used to derive general expressions, given its overconservative results and low consistency with the LS limit state actual damage of masonry infills (MIs exhibit at least an inelastic IP behaviour).

4.1 Elastic floor spectra formulation

The maximum nonstructural acceleration (1) at given floor (FL) $S_{FL}(T_{NS})_{max}$ can be evaluated as the two-step modification of PGA due to structural in-height acceleration amplification (a_H) and nonstructural dynamic interaction (a_{NS}).

$$S_{FL}(T_{NS})_{max} = PGA \cdot a_H \cdot a_{NS} = PFA \cdot a_{NS} \tag{1}$$

A bilinear expression is proposed to evaluate the a_H amplification factor (2), where z_H stands for the relative height z/H of the nonstructural component.

$$a_H = \begin{cases} 1 + \dfrac{a_{H,max} - 1}{z_H^*} z_H & for \;\; z_H < z_H^* \\ a_{H,max} & for \;\; z_H \geq z_H^* \end{cases} \tag{2}$$

Both the maximum amplification at roof level $a_{H,max}$ and height z_H^* of transition from linear to constant amplification branches can be described as functions of behaviour factor q (3), (4).

$$(z/H)^* = z_H^* = 0.4 - \frac{q}{30} \tag{3}$$

$$a_{H,max} = a_H(z_H = 1) = 2.911 \cdot q^{-0.288} \tag{4}$$

The nonstructural amplification factor a_{NS} linear expression (5) is anchored to an initial value of 3.6 and a maximum value $a_{NS,max}$ (6) at roof level that depends again on behaviour factor.

$$a_{NS} = 3.6 + (a_{NS,max} - 3.6) z_H \tag{5}$$

$$a_{NS,max} = a_{NS}(z_H = 1) = 6.745 \cdot q^{-0.28} \tag{6}$$

The proposed bilinear and linear laws are consistent with envelopes derived from nonlinear time history analyses, as depicted in Figure 4 and Figure 5. The extension of floor spectrum plateau region is strictly related to dominant frequencies and maximum fundamental period elongation. The RC structure can be divided into three zones, depending on behaviour factor q and in-height prevalence of T_1 and/or higher modes effect, evaluated though CWT transforms: higher modes zone (HMZ), mixed modes zone (MMZ) and first mode zone (FMZ). Therefore, the resonance region, delimited by aT_1 and bT_1 values, adapts to each zone, moving from the bottom to the top of the structure. The mean values of coefficients a and b as well as relative heights associated to zone transition z_{H1} and z_{H2} are calibrated on CWT results and summarised in expressions (7), (8), (9), (10). The minimum a value is equal to 0.15, given the non-negligible contribution of the third and fourth modal shapes contribution in some scenarios.

$$a = \begin{matrix} 0.15 & for\ \ z_H < z_{H2} \\ 0.60 & for\ \ z_H \geq z_{H2} \end{matrix} \tag{7}$$

$$b = \begin{matrix} 0.45 & for\ \ z_H < z_{H1} \\ 0.95 + \dfrac{q}{15} & for\ \ z_H \geq z_{H1} \end{matrix} \tag{8}$$

$$z_{H1} = 0.275 + \frac{q}{20} \tag{9}$$

$$z_{H2} = z_{H2} + 0.2 \tag{10}$$

The first branch f_I of the floor spectrum of acceleration connects PFA to the maximum nonstructural acceleration $S_{FL}(T_{NS})_{max}$, following a parabolic function (11). This shape has been selected to cover secondary acceleration peaks detected in exact spectra at higher floors, due to non-negligible higher modes influence. T_{NS} represents the elastic period of vibration of the nonstructural element.

$$f_I = PFA\left[1 + \frac{T_{NS}}{aT_1}\left(a_{NS} - 1\right)\left(2 - \frac{T_{NS}}{aT_1}\right)\right] \tag{11}$$

A Gaussian-like shape is suggested for the post-resonance third branch f_{III}, offering the opportunity to control the inflection point to cover both higher fundamental period elongation at higher levels and secondary peaks due to first mode influence at lower ones (12), (13). The γ coefficient is introduced to this purpose.

$$f_{III} = PFA \cdot a_{NS} \cdot exp\left(-\frac{1}{2}\left(\frac{\left(T_{NS} - bT_1\right)}{T_1\left(\gamma - b\right)}\right)^2\right) \tag{12}$$

$$\gamma = \begin{matrix} 1.15 + \dfrac{q}{15} - b & for\ \ z_H < z_{H1} \\ 0.40 & for\ \ z_H \geq z_{H1} \end{matrix} \tag{13}$$

Figure 8 shows an application of the proposed formulation for medium and high ductility structures, evaluating elastic floor response spectra, normalized by PGA, at five different relative heights z_H.

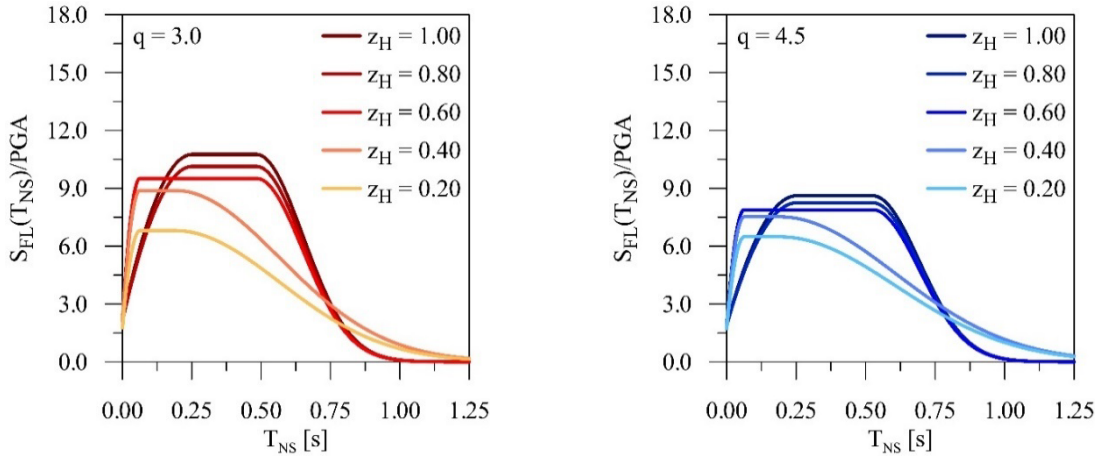

(a) Medium ductility class (MD). (b) High ductility class (HD).

Figure 8: Proposed elastic floor spectra evaluated at different heights.

4.2 Comparison of proposed and exact floor spectra for masonry infills

Maximum accelerations of MIs are collected to assemble exact infill floor response spectra, in their realistic OOP fundamental frequency domain (i.e. 0.0-0.3s, with time step 0.03s). These curves are compared to NTC18 general (G), simplified general (SG) and simplified for r.c. frames (SF) formulations as well as EC8, ASCE-SEI 41/17 and NZS1170 ones. Masonry infills behaviour factor q_{NS} is applied, depending on code provisions. For the sake of brevity, only five-storey structures are selected, focusing on the second floor (Figure 9). This position is relevant to highlight the general underestimation of floor spectra when higher modes have a significant impact on nonstructural amplification. Formulations based on modal superposition exhibit peaks close to higher modes frequencies, but acceleration values are still underestimated (this is probably due to q_{NS} overestimation). Other approaches provide an acceleration increase moving toward the fundamental period, neglecting amplification effects due to masonry infill frequency T_{MI} being closer to higher modes ones. NTC18 formulation, includes higher modes effects if T_1 exceeds 0.5s only. Despite the simpler shape, NZS1170 floor spectra provides the best matching among code expressions. This can be explained in the light of unitary MI behaviour factor.

The proposed elastic formulation is generally safe sided, since no q_{NS} value is applied. It should be compared to the $E_{IP}E_{OOP}$ and $I_{IP}E_{OOP}$ modelling assumptions only, given the common elastic OOP behaviour hypothesis (elastic spectra). In these cases, exact peaks are perfectly covered, while an obvious overestimation occurs if simplified spectra are compared to inelastic ones. The calibration of q_{NS} based on exact MIs results (q_{MI}) will be discussed in a future work.

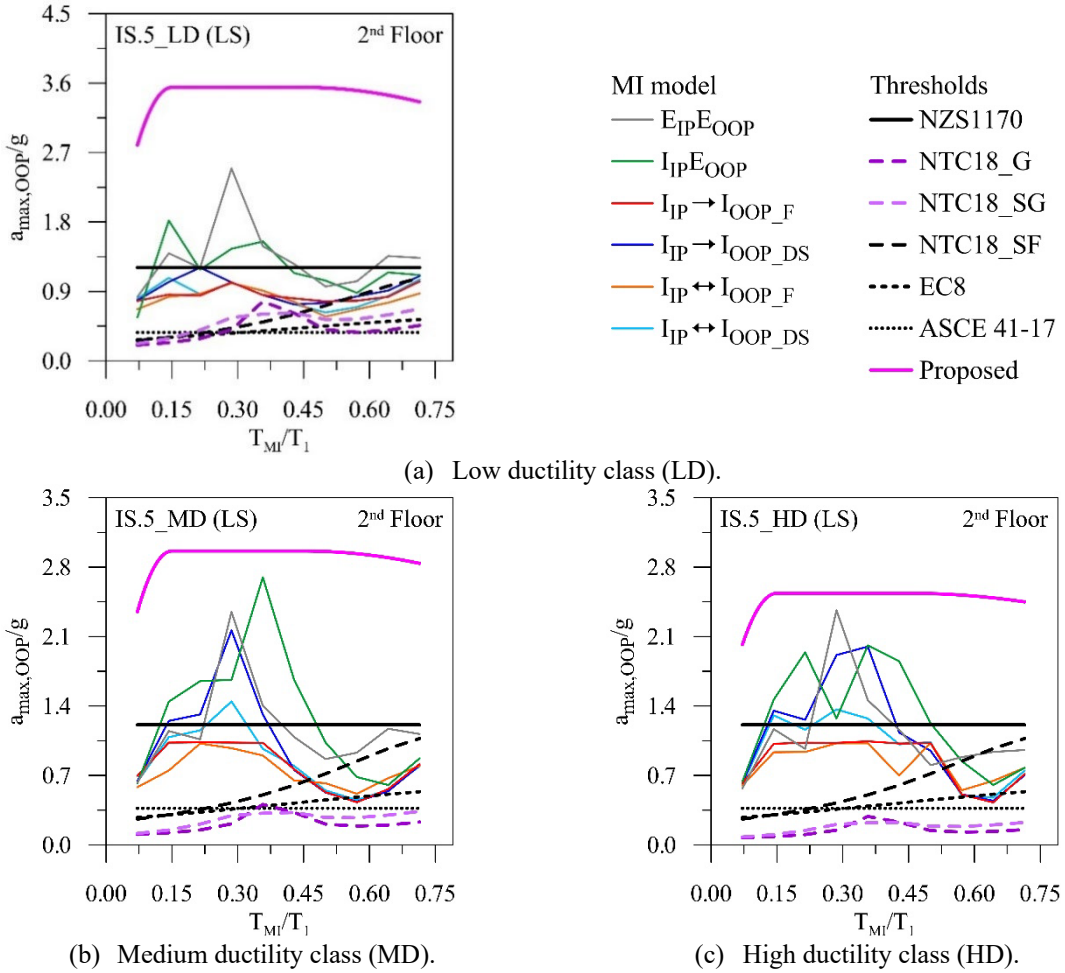

(a) Low ductility class (LD).

(b) Medium ductility class (MD).

(c) High ductility class (HD).

Figure 9: Comparison between exact, code-based MIs spectra and proposed (elastic) formulation.

5 CONCLUSIONS

A new code-oriented elastic floor spectra formulation consistent with LS seismic intensity level is proposed in this paper. The calibration procedure is based on post-processing of nodal time-histories at different structural levels for a wide set of RC totally infilled structures. A recently developed macro-model that accounts for IP and OOP inelastic responses as well as their mutual interaction is implemented in each 3D infilled frame. Various MIs response assumptions have been made to investigate their effect on rigorous elastic floor spectra. General trends for in-height and nonstructural amplification factors are derived, in order to define the peak value of floor spectra. Continuous wavelet transforms provide relevant information about the spatial contribution of fundamental and higher modes to nonstructural components motion. In this way, the elastic spectrum shape adapts to nonstructural elements position. Its first and last branches are described though rational mathematical expressions to cover secondary peaks and unforeseen above-average structural damage, that causes a higher fundamental period elongation. The preliminary comparison of this tool with exact MIs floor spectra based on post-processing of infill macro-model results shows a safe-sided prediction for elastic OOP MIs response, while a MI behaviour factor is needed to reduce the acceleration overestimation in

the case of inelastic OOP response. This topic will be discussed in detail in a future work. Code-based prescriptions do not account for the structural behaviour factor, leading to underestimated or overestimated spectrum amplification parameters a_H and a_{NS}. An overall poor prediction can be noticed if higher modes effect at lower floors is dominant, since all formulations, except NTC18 one, do not account for peaks in this spectrum area. The nonstructural behaviour factor value for MIs seems to be excessively high in the case of NTC18, EC8 (q_{MI}=2) and ASCE-SEI 41/17 (q_{MI}=1.5) simplified formulations.

REFERENCES

[1] Sullivan, T.J., Calvi, P.M., Nascimbene, R. Towards improved floor spectra estimates for seismic design. *Earthq Struct* (2013) **4(1)**:109-132.

[2] Vukobratović, V., Fajfar, P. Code-oriented floor acceleration spectra for building structures. *Bull Earthq Eng* (2017) **15**:3013-3026.

[3] NTC18. Norme Tecniche per le Costruzioni, Gazzetta Ufficiale del 20/02/2018, Supplemento ordinario n.42 (2018, in Italian).

[4] EC8 (Eurocode 8). Design of Structures for Earthquake Resistance - Part 3: Assessment and retrofitting of buildings. C.E.N., European Committee for Standardization (2004).

[5] ASCE-SEI 41/17. Seismic evaluation and retrofit of existing buildings. American Society of Civil Engineers, Virginia, USA (2017).

[6] NZSEE. The seismic assessment of existing buildings (the guidelines), Part C - Detailed seismic assessment. New Zealand Society for Earthquake Engineering (2017).

[7] Mazza, F. In-plane-out-of-plane non-linear model of masonry infills in the seismic analysis of r.c. framed buildings. *Earthq Eng Struct Dyn* (2019) **48(4)**:432-453.

[8] Naga, P., Eatherton, M.R. Analyzing the effect of moving resonance on seismic response of structures using wavelet transforms. *Earthq Eng Struct Dyn* (2014) **43**:759-768.

[9] Mazza, F., Donnici, A. In-plane-out-of-plane single and mutual interaction of masonry infills in the nonlinear seismic analysis of RC framed structures. *Eng Struct* (2022) **257(5)**:114076.

[10] Mazza, F., Donnici, A. In-plane and out-of-plane seismic damage of masonry infills in existing r.c. structures: the case study of De Gasperi-Battaglia school in Norcia. *Bull Earthq Eng* (2021) **19**:345-376.

[11] FEMA 356. Prestandard and Commentary for the Seismic Rehabilitation of Buildings. Washington, DC: Federal Emergency Management Agency (2000).

[12] Dawe, J.L., Seah, C.K. Out-of-plane resistance of concrete masonry infilled panels. *Canadian Journal of Civil Engineering* (1989) **16(6)**:854-864.

[13] Aragaw, L.F., Calvi, P. Earthquake-Induced Floor Accelerations in Base-Rocking Wall Buildings. *J Earthq Eng* (2018) **25**:941-969.

[14] Ricci, P., Di Domenico, M., Verderame, G.M. Experimental assessment of the in-plane/out-of-plane interaction in unreinforced masonry infill walls. *Eng Struct* (2018) **173**:960–978.

[15] Al-Chaar, G. Evaluating strength and stiffness of unreinforced masonry infill structures. Engineer research and development center Champaign, Illinois. CERL (2002).